P H Y S I C A L   R E V I E W   L E T T E R S

Magnetic Correlations at Graphene Edges: Basis for Novel Spintronics Devices

Oleg V. Yazyev[*]

*Ecole Polytechnique Fédérale de Lausanne (EPFL), Institute of Theoretical Physics, CH-1015 Lausanne, Switzerland
and Institut Romand de Recherche Numérique en Physique des Matériaux (IRRMA), CH-1015 Lausanne, Switzerland*

M. I. Katsnelson

Institute for Molecules and Materials, Radboud University of Nijmegen, Toernooiveld 1, 6525 ED Nijmegen, The Netherlands

Magnetic zigzag edges of graphene are considered as a basis for novel spintronics devices despite the fact that no true long-range magnetic order is possible in one dimension. We study the transverse and longitudinal fluctuations of magnetic moments at zigzag edges of graphene from first principles. We find a high value for the spin wave stiffness $D = 2100$ meV Å^2 and a spin-collinear domain wall creation energy $E_{dw} = 114$ meV accompanied by low magnetic anisotropy. Above the crossover temperature $T_x \approx 10$ K, the spin correlation length $\xi \propto T^{-1}$ limits the long-range magnetic order to ~ 1 nm at 300 K while below T_x, it grows exponentially with decreasing temperature. We discuss possible ways of increasing the range of magnetic order and effects of edge roughness on it.

Graphene, a two-dimensional form of carbon, has attracted considerable attention due to its unique physical properties and potential technological applications [1,2]. The possibility of designing graphene-based magnetic nanostructures is particularly intriguing and has been fuelled by the recent experimental observations of magnetism in graphitic materials [3,4]. A number of exceptional nanoscale spintronics devices built around the phenomenon of spin polarization localized at one-dimensional (1D) zigzag edges of graphene have been proposed [5–8]. However, feasibility of such devices is questioned by the fact that no true long-range magnetic ordering in 1D systems is possible at finite temperatures [9]. Nevertheless, nanometer range spin correlation lengths in certain 1D systems have been achieved in practice [10]. Establishing the range of magnetic order at graphene edges as well as the underlying physical mechanisms is thus crucial for practical realization of the proposed spintronics devices.

In this Letter, we study the magnetic correlations at zigzag edges of graphene by investigating the transverse and longitudinal fluctuations of magnetic moments from first principles. While the transverse excitations (spin waves) are characterized by the continuous rotation of the electron spin moments along the edge [Fig. 1(a)], the longitudinal fluctuations affect the spin correlation length only if an inversion of magnetic moments resulting in appearance of a spin-collinear domain wall [11] takes place [Fig. 1(b)]. The evaluated energies of these low-energy excitations mapped onto the classical Heisenberg or Ising models allow us to estimate the spin correlation lengths at different temperatures. Finally, possible ways of increasing the spin correlation length and the effects of edge roughness are discussed.

The first-principles calculations of the magnetic excitations are performed on the density functional theory (DFT) level using the Perdew-Burke-Ernzerhof exchange-correlation functional [12]. A noncollinear spin DFT formalism [13,14] implemented in the PWSCF plane wave pseudopotential code [15] in combination with the ultrasoft pseudopotentials [16] and a plane wave kinetic energy cutoff of 25 Ry is used to study spin wave modes. Much larger supercells are required to obtain converged results for the spin-collinear domain walls. These calculations are performed using the standard spin-polarized DFT scheme implemented in the SIESTA code [17] together with a double-ζ plus polarization basis set, an energy cutoff of 200 Ry and normconserving pseudopotentials [18]. Test calculations performed on limited size systems verify that both codes provide results in close agreement. The model systems considered are the hydrogen-terminated periodic one-dimensional graphene nanoribbons of different widths and supercell lengths relaxed in their ground state configurations.
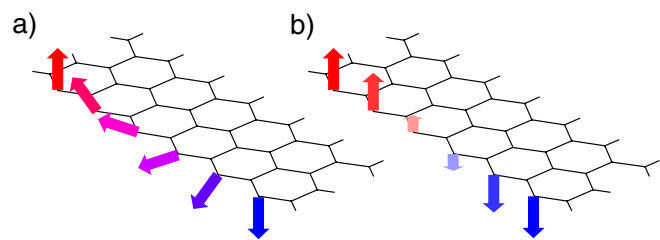

FIG. 1 (color online). Schematic representation of the transverse (a) and longitudinal (b) low-energy spin excitation at graphene zigzag edges. The magnetic moments of the outermost edge atoms are shown by arrows. The direction of magnetic moments is represented by direction of the arrows while the magnitude is illustrated through the arrow lengths.

The ground state electronic configurations of zigzag graphene nanoribbons is characterized by the ferromagnetic arrangement of spins along the edges and antiferromagnetic coupling of the spins at the opposite edges [19]. To obtain a spin-wave-excited state, we perform constrained self-consistent calculations with a penalty functional term [20] added to the total energy expression in order to induce small noncollinear deviations of the magnetization directions from the spin-collinear ground-state configuration. The total energy difference is mapped onto the quadratic spin-wave dispersion relation, $E(q) = \kappa q^2$, with $\kappa = 320$ meV Å^2. At a zigzag edge of graphene, the magnetic moments of the outermost edge atoms $m_{\text{edge}} = 0.28\ \mu_B$ while the magnetic moments localized on the atoms belonging to the A and B sublattices within a single edge unit cell are $m_A = 0.43\ \mu_B$ and $m_B = -0.13\ \mu_B$, respectively. This yields a total magnetic moment of $m = m_A + m_B = 0.30\ \mu_B$ per unit cell of zigzag edge. The obtained value of m agrees with the fact that in zigzag graphene nanoribbons, a flat band develops in one-third of the 1D Brillouin zone ($2\pi/3 \le |ka_z| \le \pi$; $a_z = 2.46$ Å is the unit cell length) when electron-electron interactions are not taken into account [21]. The spin-wave stiffness constant $D = 2\kappa/m$ turns out to be 2100 meV Å^2. Actually, this is a very high value which is about 1 order of magnitude higher than the stiffness constant of bcc iron [22,23], a three-dimensional solid with much larger magnetic moment of 2.2 μ_B per atom. Thus, our results confirm the expectation of higher spin stiffness values in magnetic materials based on sp elements compared to d element materials [24].

In sp-electron itinerant-electron magnets, Stoner-type longitudinal spin fluctuations may be essential [24]. To estimate their characteristic energy, we study collinear domain walls at the graphene zigzag edge. We have performed the calculations on a large graphene nanoribbon supercells (up to ≈ 1.8 nm wide and 6 nm long). In order to converge the self-consistent calculations to the domain wall solution, we provide an appropriate initial magnetizations of edge atoms with two equidistant domain walls per unit cell for maintaining periodicity along the nanoribbon direction. Figure 2(a) illustrates the distribution of the spin density at such a domain wall located in the center of the edge fragment shown. The spin populations of the outermost edge atoms [Fig. 2(b)] show that the domain wall is practically localized within two unit cells (0.5 nm) and the magnetization exhibits weak oscillations close to the kink. The spin-resolved projected density of states for the outermost edge atoms [Fig. 2(c)] shows an avoided crossing pattern with band gap diminishing (but not closing) at the domain wall. From the total energy difference, we find a collinear domain wall creation energy $E_{\text{dw}} = 114$ meV per edge.

In order to determine the magnetic correlation parameters in the presence of spin wave fluctuations, we recall the
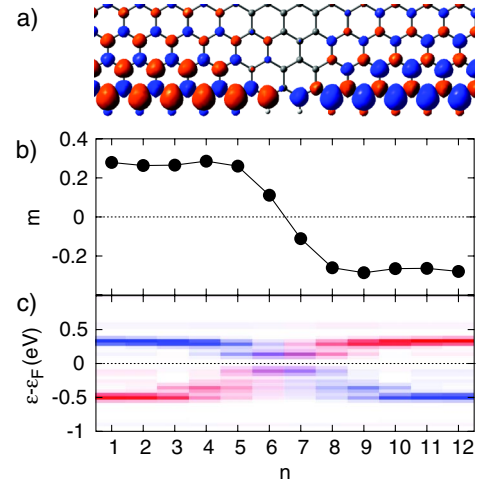

FIG. 2 (color online). (a) Spin density isosurface plot for the collinear domain wall excitation at a zigzag edge of graphene. Light gray (red) and dark gray (blue) surfaces correspond to spin-up and spin-down electrons, respectively. Spin populations m (b) and spin-resolved projected density of states (c) for the outermost edge atoms. The edge atoms are numbered with n.

nearest-neighbor 1D classical Heisenberg model

$$H = -a\sum_i \hat{\mathbf{s}}_i \hat{\mathbf{s}}_{i+1} - d\sum_i \hat{s}_i^z \hat{s}_{i+1}^z - m\mathbf{H}\sum_i \hat{\mathbf{s}}_i, \qquad (1)$$

where $\hat{\mathbf{s}}_i$ is the magnetic moment unit vector at site i and $\mathbf{H}$ is the external magnetic field vector. The Heisenberg coupling $a = 2\kappa/a_z^2 = 105$ meV corresponds to the value of κ calculated above from first principles. The axial anisotropy parameter d is expected to be small due to intrinsically weak spin-orbit coupling in graphene [25,26]. We obtain an-order-of-magnitude estimate for the magnetic anisotropy $d/a = 10^{-4}$ using the spin-orbit coupling strength of ~ 0.01 meV [25] predicted for graphene with weak corrugations observed experimentally [27,28]. The estimated d/a agrees with the recent measurements of 2D magnetic correlations in irradiated graphite [29] and with the electron spin resonance g-tensor anisotropies in graphitic molecular radicals [30,31].

The spin correlation length ξ^α ($\alpha = x, y, z$) defines the decay law of the spin correlation function $\langle \hat{s}_i^\alpha \hat{s}_{i+l}^\alpha \rangle = \langle \hat{s}_i^\alpha \hat{s}_i^\alpha \rangle \exp(-l/\xi^\alpha)$, i.e., the range of magnetic order. First, we evaluate the zero-field spin correlation length due to the transverse spin fluctuations as a function of temperature (see Fig. 3) [32]. Above the crossover temperature $T_x = \sqrt{ad} \approx 10$ K [33], the small anisotropy term of the model Hamiltonian has practically no influence, and the system exhibits behavior typical for an isotropic Heisenberg model [34] with $\xi_{\text{sw}}^\alpha \approx 300/T$ [nm] and $\langle \hat{s}_i^\alpha \hat{s}_i^\alpha \rangle = 1/3$. Below T_x, the anisotropy term starts playing an important role, and the solution exhibits a characteristic for 1D Ising model exponential divergence of $\xi_{\text{sw}}^z \propto \exp(\sqrt{8ad}/kT)$ and $\langle \hat{s}_i^z \hat{s}_i^z \rangle = 1$ for $T \to 0$ K. The spin cor-
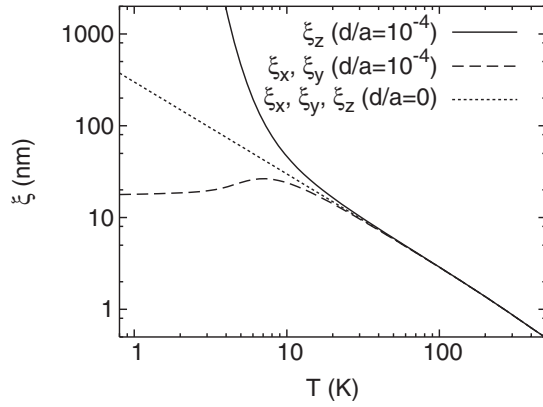
FIG. 3. Correlation lengths of magnetization vector components orthogonal (ξ_z) and parallel (ξ_x, ξ_y) to the graphene plane as a function of temperature T for weakly anisotropic ($d/a = 10^{-4}$) and isotropic ($d/a = 0$) Heisenberg models.

relation length at zero field in the presence of spin-collinear domain walls is the one for 1D Ising model, $\xi_{dw}^\alpha \approx \exp(E_{dw}/kT)$. Since $E_{dw} \gg \sqrt{8ad}$ [33], the overall spin correlation length ξ in the presence of both transverse and longitudinal fluctuations, $\xi^{-1} = \xi_{sw}^{-1} + \xi_{dw}^{-1} \approx \xi_{sw}^{-1}$, is defined predominantly by the spin wave disorder.

At room temperature (~ 300 K), the spin correlation length $\xi = 3.7$ unit cells (~ 1 nm). This result implies that a spintronics device based on magnetic graphene edges can be operated at room temperature only if its dimensions do not exceed several spin correlation lengths, i.e., several nanometers. The device dimensions can be scaled linearly by lowering the operation temperature, and below T_x, this size could be extended beyond the micrometer scale. These estimations may first look rather disappointing, but nevertheless they are comparable to one of the most appealing examples of 1D magnetism: monoatomic Co chains on Pt substrate characterized by a ferromagnetic order range of ≈ 4 nm at 45 K [10]. In this d-element system, ferromagnetic order stems mainly from the anomalously high magnetic anisotropy which is absent in graphene nanostructures. However, the lack of anisotropy is partially compensated by the high spin stiffness which results in considerable spin correlation lengths even in the isotropic regime above T_x. While the spin stiffness constant can hardly be increased, we suggest several ways of increasing the magnetic anisotropy (and thus T_x) by strengthening the spin-orbit coupling through increasing curvature, applying external electric field or coupling graphene to a substrate [25]. Alternatively, the magnetic anisotropies can be increased by chemical functionalization of graphene edges with heavy element functional groups (e.g., iodine) coupled to the spin-polarized edge states via the exchange polarization [35,36]. Augmenting the crossover temperature above 300 K would result in a significant increase of ξ^z to the length scales of the present-day semiconductor technology.

Thus, the graphene edges at finite temperatures are not actually ferromagnetic but superparamagnetic ones. For the isotropic Heisenberg model, the enhancement factor for the susceptibility in comparison with one of noninteracting spins reads [34]

$$\frac{\chi}{\chi_0} = \frac{1+u}{1-u} \approx \frac{2a}{T} \qquad (2)$$

where $u = \coth(a/T) - T/a$ and the approximation being valid at $a \gg T$. At room temperature, the susceptibility enhancement factor $\chi/\chi_0 \approx 8$.

Although we found a relatively high value of E_{dw}, the localized domain walls may become energetically more favorable at edge defects, and therefore we discuss creation of localized domain walls at different types of topological imperfections at zigzag graphene edge classified as shown in Fig. 4. The simplest case of edge roughness is a boundary atom missing from the π-conjugation network [Fig. 4(b)]. Such sp^2-vacancy formation may result from the rehybridization of an outermost atom into the sp^3 state due to chemical modification or because of the creation of a true vacancy. The domain wall creation energy at an sp^3-hybridized atom is found to be 24 meV, i.e., factor of 5 smaller than $E_{dw} = 114$ meV for the ideal zigzag edge. Such decrease will have a dramatic effect on the long-range magnetic order at room temperature since E_{dw} is lowered to kT (≈ 25 meV at 300 K). An even more dramatic decrease to 4 meV is observed at the Stone-Wales defect [Fig. 4(c)], a topological structure obtained by the 90°-rotation of a single C–C bond which locally breaks the bipartite lattice symmetry. The presence of an edge step [Fig. 4(d)] has a less severe effect and reduces E_{dw} to 62 meV. A completely different situation is observed for a 120°-turn of the zigzag edge [Fig. 4(e)]. The antiferromagnetic arrangement of spins at the edge segments separated by the 120°-turn is by 22 meV more stable than the ferromagnetic arrangement. This is due to the change of bipartite sublattice to which belong the outermost edge atoms and due to the antiferromagnetic coupling between the magnetic moments in different sublattices [37,38]. Similar behavior has recently been pointed out for the
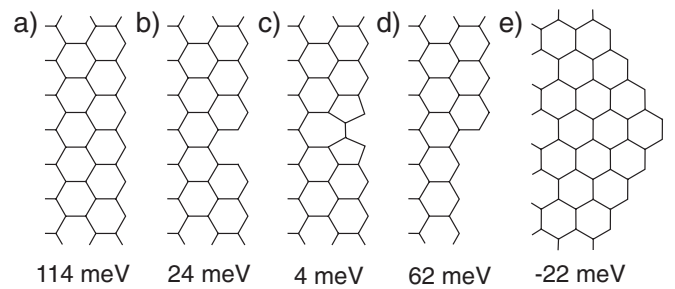

FIG. 4. Ideal zigzag edge of graphene (a) and various types of edge defects: missing or rehybridized edge atom (b), Stone-Wales defect (c), edge step (d), and 120° edge turn. The domain wall creation energies at these structures are shown.

edges of hexagonal graphene nanoislands [39]. Domain walls are thus naturally pinned to such turns, although the energy difference is close to kT at room temperature. A "spin-inverter" device design based on such a 120°-turn topology can be anticipated. Simple chemical modifications which do not perturb the π conjugation network at graphene edges show almost no effect on E_{dw}. For an ideal zigzag edge terminated with electronegative fluorine atoms, we find $E_{dw} = 117$ meV very close to the value for the hydrogen-terminated edge (114 meV).

To conclude, we have studied from first principles the energetics of transverse and longitudinal spin fluctuations at the one-dimensional magnetic zigzag edge of graphene. The transverse fluctuations characterized by the high spin stiffness constant are the main limiting factor of the spin correlation length which is found to be ~ 1 nm at room temperature. For the temperatures above ~ 10 K, the spin correlation length is inversely proportional to the temperature due to the low magnetic anisotropy of the system. Below the crossover temperature, the spin correlation length grows exponentially with decreasing temperature. We propose several approaches for extending the range of magnetic order by increasing the magnetic anisotropy in this carbon-based system and discuss the effect of edge roughness on the spin correlation length.

---

*oleg.yazyev@epfl.ch

[1] A. K. Geim and K. S. Novoselov, Nat. Mater. **6**, 183 (2007).
[2] M. I. Katsnelson, Mater. Today **10**, 20 (2007).
[3] P. Esquinazi, D. Spemann, R. Höhne, A. Setzer, K.-H. Han, and T. Butz, Phys. Rev. Lett. **91**, 227201 (2003).
[4] H. Ohldag, T. Tyliszczak, R. Höhne, D. Spemann, P. Esquinazi, M. Ungureanu, and T. Butz, Phys. Rev. Lett. **98**, 187204 (2007).
[5] Y.-W. Son, M. L. Cohen, and S. G. Louie, Nature (London) **444**, 347 (2006).
[6] L. Brey, H. A. Fertig, and S. Das Sarma, Phys. Rev. Lett. **99**, 116802 (2007).
[7] M. Wimmer, I. Adagideli, S. Berber, D. Tománek, and K. Richter, arXiv:0709.3244.
[8] See also N. Tombros, C. Jozsa, M. Popinciuc, H. T. Jonkman, and B. J. van Wees, Nature (London) **448**, 571 (2007).
[9] N. D. Mermin and H. Wagner, Phys. Rev. Lett. **17**, 1133 (1966).
[10] P. Gambardella, A. Dallmeyer, K. Maiti, M. C. Malagoli, W. Eberhardt, K. Kern, and C. Carbone, Nature (London) **416**, 301 (2002).

[11] K. Wakabayashi and K. Harigaya, J. Phys. Soc. Jpn. **72**, 998 (2003).
[12] J. P. Perdew, K. Burke, and M. Ernzerhof, Phys. Rev. Lett. **77**, 3865 (1996).
[13] T. Oda, A. Pasquarello, and R. Car, Phys. Rev. Lett. **80**, 3622 (1998).
[14] R. Gebauer and S. Baroni, Phys. Rev. B **61**, R6459 (2000).
[15] S. Baroni it et al., http://www.pwscf.org/.
[16] D. Vanderbilt, Phys. Rev. B **41**, 7892 (1990).
[17] J. M. Soler et al., J. Phys. Condens. Matter **14**, 2745 (2002).
[18] N. Troullier and J. L. Martins, Phys. Rev. B **43**, 1993 (1991).
[19] H. Lee, Y.-W. Son, N. Park, S. Han, and J. Yu, Phys. Rev. B **72**, 174431 (2005).
[20] The penalty term $E^p = \lambda \sum_i \{[\hat{m}_{ix} - \cos(\theta_i)\sin(\phi_i)]^2 + [\hat{m}_{iy} - \sin(\theta_i)\sin(\phi_i)]^2 + [\hat{m}_{iz} - \cos(\phi_i)]^2\}$ used in this work induces a precession-like arrangement of spins along the graphene edge by constraining the magnetic moment direction $\hat{\mathbf{m}}_i$ of each carbon atom i. The deviation angle $\phi_i = \Phi$ if atom i belongs to sublattice A and $\phi_i = \Phi + \pi$ otherwise. The angle θ_i varies with the fractional coordinate a_i of the 1D supercell as $\theta_i = 2\pi a_i$. The resulting magnitude of spin stiffness D is stable against the choice of λ and Φ equal here to 10 Ry and $\pi/36$, respectively.
[21] K. Nakada, M. Fujita, G. Dresselhaus, and M. S. Dresselhaus, Phys. Rev. B **54**, 17954 (1996).
[22] J. W. Lynn, Phys. Rev. B **11**, 2624 (1975).
[23] M. V. You, V. Heine, A. J. Holden, and P. J. Lin-Chung, Phys. Rev. Lett. **44**, 1282 (1980).
[24] D. M. Edwards and M. I. Katsnelson, J. Phys. Condens. Matter **18**, 7209 (2006).
[25] D. Huertas-Hernando, F. Guinea, and A. Brataas, Phys. Rev. B **74**, 155426 (2006).
[26] H. Min, J. E. Hill, N. A. Sinitsyn, B. R. Sahu, L. Kleinman, and A. H. MacDonald, Phys. Rev. B **74**, 165310 (2006).
[27] S. V. Morozov, K. S. Novoselov, M. I. Katsnelson, F. Schedin, L. A. Ponomarenko, D. Jiang, and A. K. Geim, Phys. Rev. Lett. **97**, 016801 (2006).
[28] J. C. Meyer, A. K. Geim, M. I. Katsnelson, K. S. Novoselov, T. J. Booth, and S. Roth, Nature (London) **446**, 60 (2007).
[29] J. Barzola-Quiquia, P. Esquinazi, M. Rothermel, D. Spemann, T. Butz, and N. García, Phys. Rev. B **76**, 161403(R) (2007).
[30] A. J. Stone, Mol. Phys. **7**, 311 (1964).
[31] B. G. Segal, A. Reymond, and G. K. Fraenkel, J. Chem. Phys. **51**, 1336 (1969).
[32] G. S. Joyce, Phys. Rev. Lett. **19**, 581 (1967).
[33] A. C. Faria and A. T. Pires, J. Phys. C **12**, 2637 (1979).
[34] M. E. Fisher, Am. J. Phys. **32**, 343 (1964).
[35] D. A. Goodings, Phys. Rev. **123**, 1706 (1961).
[36] O. V. Yazyev, arXiv:cond-mat/0702424.
[37] E. H. Lieb, Phys. Rev. Lett. **62**, 1201 (1989).
[38] O. V. Yazyev and L. Helm, Phys. Rev. B **75**, 125408 (2007).
[39] J. Fernández-Rossier and J. J. Palacios, Phys. Rev. Lett. **99**, 177204 (2007).